J. Plasma Physics (2010), *vol.* 76, *part* 2, *pp.* 169–181.
doi:10.1017/S0022377810000024

Nonlinear modulation of ion-acoustic waves in two-electron-temperature plasmas

A. ESFANDYARI-KALEJAHI[1], I. KOURAKIS[2] and M. AKBARI-MOGHANJOUGHI[1]

[1] Department of Physics, Faculty of Science, Azarbaijan University of Tarbiat Moallem, 51745-406, Tabriz, Iran
(ra-esfandyari@azaruniv.edu)

[2] Department of Physics and Astronomy, Centre for Plasma Physics, Queen's University Belfast, BT7 1NN, Northern Ireland, UK

(Received 19 April 2009, revised 7 September 2009 and accepted 31 December 2009)

Abstract. The amplitude modulation of ion-acoustic waves is investigated in a plasma consisting of adiabatic warm ions, and two different populations of thermal electrons at different temperatures. The fluid equations are reduced to nonlinear Schrödinger equation by employing a multi-scale perturbation technique. A linear stability analysis for the wave packet amplitude reveals that long wavelengths are always stable, while modulational instability sets in for shorter wavelengths. It is shown that increasing the value of the hot-to-cold electron temperature ratio (μ), for a given value of the hot-to-cold electron density ratio (ν), favors instability. The role of the ion temperature is also discussed. In the limiting case $\nu = 0$ (or $\nu \to \infty$), which correspond(s) to an ordinary (single) electron-ion plasma, the results of previous works are recovered.

1. Introduction

Plasmas are often characterized by a coexistence of cold and hot electron populations. Such two-electron-temperature (2eT) plasmas occur in hot cathode discharge plasma experiments [1,2], in thermonuclear fusion [3,4] and in RF-produced plasmas in ELMO confinement devices [5]. Various spacecraft observations, e.g. by the FAST at the auroral region [6, 7], S3-3 [8], Viking [9, 10] and GEOTAIL and POLAR [7, 11] missions have reported the occurrence of 2eT plasmas in the magnetosphere and have recorded localized potential excitations propagating in them.

The nonlinear behavior of ion-acoustic (IA) solitary waves has been long studied quite exhaustively, both theoretically (see e.g. in [12–14] and references therein) and experimentally [14–16]. Naturally, the properties of IA excitations are considerably affected by the simultaneous presence of cold and hot electrons, both in the linear [2] and in the nonlinear (see e.g. Refs. 17–21) regime(s). Interestingly, both positive and negative IA potential perturbation (IA solitons) can propagate in 2eT plasmas [22–24], unlike electron-ion plasma (*e-i*) plasmas, which only support positive potential disturbances [14]. As expected, the dynamics of IA solitons in 2eT plasma depends on the relative temperature and density ratio(s) between the

two electron components [17], which also affect the very conditions for existence of solitary excitations.

Beyond soliton theories (e.g. of the Korteweg-de Vries type [14]), which dominate weakly dispersive ion-acoustic waves (IAW), shorter carrier wavelength wave packets are described by nonlinear Schrödinger (NLS)-type [25, 26] perturbative theories, which provide the modulational (in)stability profile of their envelope and model the dynamics of envelope soliton structures at the first stage after their formation. The addition of a small fraction of cold electrons in *e-i* plasma can drastically affect the modulational dynamics of IA wave packets [27], and may also their response to oblique perturbations [28–30].

Recently, 2eT plasmas appear to have received new theoretical interest, as witnessed by an increasing number of studies on various plasma modes in such plasmas in the last decade. The co-existence of cold and hot electrons has been revisited with respect to ion-acoustic [31, 32] and electron-acoustic [33] pulses and double layers, surface electron-acoustic waves in dusty plasmas [34], multi-dimensional ES solitons in electron-positron plasmas [35], quantum plasmas [36], to mention only a few. Space observations have also attracted interest in the high-frequency electron modes in 2eT plasmas [37, 38], not overlooking related amplitude modulation studies [39, 40].

Our scope here is to revisit the modulational dynamics of electrostatic wave packets in 2eT plasmas. We shall investigate the occurrence of envelope solitary excitations, associated with the modulational instability of IAWs propagating in a collisionless plasma consisting of adiabatic warm ions and electrons. Relying on a standard multi-scale perturbation technique [12, 25], we shall obtain a NLS-type equation [26] for the wave amplitude, to study its dynamics. The layout of this paper is as follows. In Sec. 2, a fluid-plasma analytical model is introduced. Section 3 is devoted to the derivation of the NLS Equation (NLSE) for the wave amplitude dynamics and to a discussion of the linear stability of the IAW envelope. A parametric analysis of the stability of the wave packet envelope in terms of plasma parameters is given in Sec. 5. Finally, the conclusion is given in Sec. 6.

2. Basic equations

In a plasma, which consists of warm ions, hot and cold electrons, the basic set of one-dimensional (1D) fluid equations can be written as

$$\frac{\partial n_i}{\partial t} + \frac{\partial \left(n_i u_i\right)}{\partial x} = 0, \tag{2.1}$$

$$\frac{\partial u_i}{\partial t} + u_i \frac{\partial u_i}{\partial x} + \frac{Z_i e}{m_i} \frac{\partial \phi}{\partial x} + \frac{1}{n_i m_i} \frac{\partial p_i}{\partial x} = 0, \tag{2.2}$$

$$\frac{\partial p_i}{\partial t} + u_i \frac{\partial p_i}{\partial x} + 3 p_i \frac{\partial u_i}{\partial x} = 0, \tag{2.3}$$

$$\frac{\partial^2 \phi}{\partial^2 x} = 4\pi e \left(n_c + n_h - z_i n_i\right), \tag{2.4}$$

where n_i, n_c and n_h are ion, cold and hot electron densities, respectively. The variables s, u_i, p_i and ϕ respectively denote the ion fluid-velocity, ion fluid-pressure and the corresponding electrostatic potential. Parameters Z_i and m_i are ions' atomic number and mass. Both, electron species (cold and hot) are taken to follow

the Boltzmann distribution, that is

$$n_c = n_{c0} e^{\frac{e\phi}{K_B T_c}}, \qquad n_h = n_{h0} e^{\frac{e\phi}{K_B T_h}}. \tag{2.5}$$

Here, T_c and T_h represent the cold and hot electron temperatures, respectively, and the zero subscript denotes the equilibrium values. The right-hand side of (2.4), then, cancels out at equilibrium situation due to the overall neutrality condition, giving rise to the following expression:

$$n_{c0} + n_{h0} - Z_i n_{i0} = 0. \tag{2.6}$$

The variables, time (t) and space (x), are normalized with respect to the ion plasma period (inverse frequency) defined by $\omega_p^{-1} = (4\pi n_{i0} Z_i^2 e^2/m_i)^{-1/2}$ and the corresponding effective Debye radius $r_{D,eff} = (K_B T_{eff}/4\pi n_{i0} Z_i e^2)^{1/2}$. We also normalize densities n_i, n_c and n_h to $n_i 0$ and the pressure p to $p_{i0} = n_{i0} K_B T_{i0}$. Electrostatic potential ϕ is scaled to $\phi_0 = K_B T_{eff}/e$ and the velocity u_i to ion-acoustic speed $c_{s,eff} = (K_B T_{eff} Z_i/m_i)^{1/2}$. Here, T_{eff} is the effective temperature $T_{eff} = (n_{h0} + n_{c0})/(n_{h0}/T_h + n_{c0}/T_c)$.

Equations (2.1)–(2.4) can thus be combined into a set of reduced (dimensionless) relations, which are as follows:

$$\frac{\partial n_i}{\partial t} + \frac{\partial (n_i u_i)}{\partial x} = 0, \tag{2.7}$$

$$\frac{\partial u_i}{\partial t} + u_i \frac{\partial u_i}{\partial x} + \frac{\partial \phi}{\partial x} + \frac{h}{n_i} \frac{\partial p_i}{\partial x} = 0, \qquad h = \frac{\sigma}{Z_i} \tag{2.8}$$

$$\frac{\partial p_i}{\partial t} + u_i \frac{\partial p_i}{\partial x} + 3p_i \frac{\partial p_i}{\partial x} = 0, \tag{2.9}$$

$$\frac{\partial^2 \phi}{\partial x^2} = 1 + \left(\phi + \alpha\phi^2 + \alpha'\phi^3\right) - n_i. \tag{2.10}$$

All quantities in the preceding equations (and everywhere below) are dimensionless; to be distinguished from the homologous ones in (2.7)–(2.10) by a tilde, say, here omitted for clarity. The parameter σ denotes the ratio of ion temperature to the effective temperature ($\sigma = T_i/T_{eff}$). The dimensionless parameters, α and α', are related to the fractional electron temperature ($\mu = T_h/T_c$) and densities ($\nu = n_{h0}/n_{c0}$) with the following expressions:

$$\alpha = \frac{1}{2} \frac{(1+\nu)\left(\nu + \mu^2\right)}{(\nu+\mu)^2}, \quad \alpha' = \frac{1}{6} \frac{(1+\nu)^2\left(\nu + \mu^3\right)}{(\nu+\mu)^3}. \tag{2.11}$$

Note that $\alpha \to 1/2$ and $\alpha' \to 1/6$ in the ordinary electron-ion plasma limit ($\nu \to 0$). Although $Z_i = 1$ can be assumed in the forthcoming algebra, in order for our results to be compared to the existing ones, here we keep Z_i arbitrary for generality.

3. Perturbation analysis for the wave packet amplitude

In order to obtain an explicit evolution equation, describing the propagation of modulated electrostatic envelopes, from the basic model (2.7)–(2.10), we shall employ the standard reductive perturbation (multiple scales) technique [12, 25]. The independent time (t) and coordinate (x) variables are stretched as $\tau = \varepsilon^2 t$ and $\xi = \varepsilon(x - \lambda t)$, in which ε represents a small (real) perturbation parameter and λ

denotes the phase velocity, to be determined by the compatibility requirements. We define a vector for the corresponding state quantities $\boldsymbol{S}$, which is a (column) vector $(n_i, p_i, u_i, \phi)\dagger$, defined as:

$$\mathbf{S} = \mathbf{S^{(0)}} + \sum_{n=1}^{\infty} \varepsilon^n \mathbf{S^{(n)}},$$

in which the $\mathbf{S^{(0)}}$ is a (column) vector $(1, 1, 0, 0)$ and

$$\mathbf{S}^{(n)} = \sum_{l=-\infty}^{+\infty} \mathbf{S_l}^{(n)}(\xi, \tau) e^{il(kx-\omega t)}.$$

Here, k and ω denote the (fast) fundamental-phase variables, i.e. the dimensionless carrier wave number and frequency (scaled by $2\pi/r_D$ and ω_p), respectively. All variables satisfy the reality condition $\boldsymbol{S_l^{(n)} = S_{-l}^{(n)*}}$, where the superscript star denotes the complex conjugate (*c.c.*).

Substituting the above expansion into (2.7)–(2.10) and making use of stretched variables, we may now isolate distinct orders in ε.

The *first*-order reduced equations are

$$\begin{aligned} -i\omega n_{i,l}^{(1)} + iku_{i,l}^{(1)} &= 0, \\ -i\omega u_{i,l}^{(1)} + ik\phi_{i,l}^{(1)} + ik\sigma p_{i,l}^{(1)} &= 0, \\ -i\omega p_{i,l}^{(1)} + 3iku_{i,l}^{(1)} &= 0, \\ (1-k^2)\phi_l^{(1)} &= n_{i,l}^{(1)}. \end{aligned} \tag{3.1}$$

Consequently, (3.1) yield

$$\omega^2 = 3k^2\sigma + \frac{k^2}{1+k^2}. \tag{3.2}$$

This is the dispersion relation for IAWs in ordinary electron-ion plasmas (i.e. for a single electron population in the background), yet note that the details of our plasma composition here are 'hidden' in the normalization above. Thus, the dispersion relation (3.2) is similar to the one derived in [42], and also reduces to the expression given by Sharma and Buti [27] in the cold-ion limit. The *first*-order harmonic amplitudes in terms of potential components are determined by the following relations:

$$n_{i,1}^{(1)} = N_{1,1}\phi_1^{(1)}, \quad u_{i,1}^{(1)} = U_{1,1}\phi_1^{(1)}, \quad p_{i,1}^{(1)} = P_{1,1}\phi_1^{(1)}, \tag{3.3}$$

where

$$N_{1,1} = \tfrac{k^2}{\omega^2 - 3k^2\sigma}, \quad U_{1,1} = \tfrac{k\omega}{\omega^2 - 3k^2\sigma}, \quad P_{1,1} = \tfrac{3k^2}{\omega^2 - 3k^2\sigma}. \tag{3.4}$$

From the second-order ($n = 2$) equations for the *1st* harmonics ($l = 1$), one can deduce the following compatibility relation:

$$\lambda = \frac{\omega}{k} - \frac{(\omega^2 - 3k^2\sigma)^2}{k\omega}. \tag{3.5}$$

It is easily shown that $\lambda = v_g(k) = \partial\omega/\partial k$, therefore the parameter λ corresponds to the group velocity in the (x) direction of modulation.

The second-order *1st* harmonic quantities have the form

$$\begin{aligned} n_{i,1}^{(2)} &= N_{2,1}\frac{\partial\phi_1^{(1)}}{\partial\xi} + N_{1,1}\phi_1^{(2)}, \\ u_{i,1}^{(2)} &= U_{2,1}\frac{\partial\phi_1^{(1)}}{\partial\xi} + U_{1,1}\phi_1^{(2)}, \\ p_{i,1}^{(2)} &= P_{2,1}\frac{\partial\phi_1^{(1)}}{\partial\xi} + P_{1,1}\phi_1^{(2)}, \end{aligned} \tag{3.6}$$

where

$$\begin{aligned} N_{2,1} &= \frac{2\omega k(\omega - k\lambda)}{(\omega^2 - 3k^2\sigma)^2}, \\ U_{2,1} &= \frac{(\omega - k\lambda)(\omega^2 + 3k^2\sigma)}{(\omega^2 - 3k^2\sigma)^2}, \\ P_{2,1} &= \frac{6k\omega(\omega - k\lambda)}{(\omega^2 - 3k^2\sigma)^2}. \end{aligned} \tag{3.7}$$

The second harmonic mode of the carrier wave comes from the nonlinear self-interaction part, which is obtained in terms of $(\phi_1^{(1)})^2$ component. The component of $l = 2$ for the second-order ($n = 2$) reduced equations determine the second harmonic quantities, which are

$$\begin{aligned} n_{i,2}^{(2)} &= N_{2,2}\left(\phi_1^{(1)}\right)^2, u_{i,2}^{(2)} = U_{2,2}\left(\phi_1^{(1)}\right)^2, \\ p_{i,2}^{(2)} &= P_{2,2}\left(\phi_1^{(1)}\right)^2, \phi_2^{(2)} = \Phi_{2,2}\left(\phi_1^{(1)}\right)^2. \end{aligned} \tag{3.8}$$

The second-order coefficients in (3.8) are presented in Appendix A. A zeroth harmonic mode also appears due to the self-interaction of the modulated carrier wave. However, the corresponding expression cannot be fully determined within the second orders and requires considering the third-order equation sets. Therefore, the $l = 0$ components of the third-order ($n = 3$) part of the reduced equations determine the following second-order amplitudes of the zero harmonic mode as

$$\begin{aligned} n_{i,0}^{(2)} &= N_{2,0}\left|\phi_1^{(1)}\right|^2, \quad u_{i,0}^{(2)} = U_{2,0}\left|\phi_1^{(1)}\right|^2, \\ p_{i,0}^{(2)} &= P_{2,0}\left|\phi_1^{(1)}\right|^2, \quad \phi_0^{(2)} = \Phi_{2,0}\left|\phi_1^{(1)}\right|^2. \end{aligned} \tag{3.9}$$

The expressions for the coefficients in (3.9) are presented in Appendix B.

Continuing into $n = 3$ and $l = 1$ orders, the condition for suppression of secular terms leads to the following NLSE

$$i\frac{\partial\psi}{\partial\tau} + P\frac{\partial^2\psi}{\partial\xi^2} + Q\left|\psi\right|^2\psi = 0\,. \tag{3.10}$$

This equation describes the slow evolution of the first-order amplitude of the plasmas perturbed potential $\phi \equiv \phi_1^{(1)}$. The lengthy expressions for the dispersion coefficient P and the nonlinear coefficient Q are given in Appendix C. We note that the dispersion coefficient P is related to the dispersion curve as $P = \partial^2\omega/2\partial k^2$.

A short algebraic manipulation shows that the dispersion coefficient P, given in (C 1), is the same as the one derived in [42]. It is straightforward to check that the coefficient P is always negative for all parameter values of interest to us here.

For $\sigma = 0$, the coefficient P reduces to the one given in [27] and P is always negative for all k.

The nonlinear coefficient Q expresses the nonlinearity, which is due to the carrier wave self-interaction.

As we shall discuss below, the sign of the nonlinear coefficient Q (C 2) determines whether the wave packet is stable (for $Q > 0$) or not ($Q < 0$). For different values of ν, μ and σ, the critical wave number k_{cr}, for which the modulation instability appears, can be obtained from the equation $Q(k_{cr}, \alpha, \alpha', \sigma) = 0$ by solving numerically (see in Sec. 5 below). It is pointed out that near the critical value k_{cr}, the nonlinearity coefficient Q has a small value, hence (3.10) becomes linear and no localized excitation can be obtained. In this case one must consider higher-order nonlinearities, neglected here.

For the sake of gaining some analytical insight in dynamics, the investigation of behavior of the coefficients P and Q in the case of long wavelengths, i.e. $k \ll 1$, can be of interest. In the limit $k \ll 1$, the dispersion relation (3.2) reduces to $\omega \approx k\sqrt{1+3\sigma}$. The coefficients P and Q are then given by

$$\begin{aligned} P &\approx -\frac{3}{2}\frac{k}{\sqrt{1+3\sigma}}, \\ Q &\approx \frac{(144\sigma - 48\alpha + 72)\sigma + (2\alpha - 3)^2}{12k\sqrt{1+3\sigma}}. \end{aligned} \tag{3.11}$$

In the cold ion limit, for $\sigma = 0$, we have

$$\begin{aligned} P &\approx -\frac{3}{2}k, \\ Q &\approx \frac{(2\alpha - 3)^2}{12k}, \end{aligned} \tag{3.12}$$

which coincides with the result in [28]. We note, comparing the latter two expressions, the important role played by σ in the value and the sign of Q.

4. Stability analysis – characteristics of envelope excitations

The stability analysis of the NLS (3.10) consists in linearizing around the monochromatic wave solution $\psi = \hat{\psi}\, e^{iQ|\hat{\psi}|^2\tau}$, i.e. setting $\hat{\psi} = \hat{\psi}_0 + \varepsilon\hat{\psi}_1$, and then taking the perturbed $\hat{\psi}_1$ to be of the general form $\hat{\psi}_1 = \hat{\psi}_{1,0}e^{i(\hat{k}\xi - \hat{\omega}\tau)}$ (the perturbation wave number $\hat{k}$ and the frequency $\hat{\omega}$ should be distinguished from the similar carrier wave quantities k and ω). The dispersion relation

$$\hat{\omega}^2 = P\hat{k}^2\ (P\hat{k}^2 - 2Q|\hat{\psi}_0|^2)$$

is then obtained. It is obvious that in order for the wave amplitude to be stable, the value of the product PQ should be negative. Conversely, for positive PQ values, instability sets in for perturbation wave numbers below a critical value defined by $\hat{k}_{cr} = \sqrt{2|Q/P|}\ |\hat{\psi}_0|$, i.e. for wavelengths above a threshold value $\lambda_{cr} = 2\pi/\hat{k}_{cr}$. The maximum instability growth rate is $\sigma = |\mathrm{Im}\hat{\omega}(\hat{k})|\sigma_{\max} = |\mathrm{Im}\hat{\omega}|_{\hat{k}=\hat{k}_{cr}/\sqrt{2}} = |Q||\hat{\psi}_0|^2$, which is achieved for $\hat{k} = \hat{k}_{cr}/\sqrt{2}$.

Arbitrary amplitude localized solutions of the NLS (3.10) can be found in the form of bright and dark (gray/black) envelope solitons. Exact expressions for these envelope structures are deduced by substituting $\phi = \sqrt{\rho}\exp i\theta$ into (3.10) (where ρ and θ are both real), and separating real and imaginary parts. The detailed derivation is exposed in [25, 41]; therefore, we shall only provide a brief outline of the properties of envelope solitons and relevant quantities in the following.

A bright-type solution (bright envelope soliton) is obtained for the positive values of the coefficient product PQ, i.e. for $Q < 0$ here. This solution represents a localized amplitude pulse, which contains (modulates) the fast carrier wave oscillation. These bell-shaped excitations (vanishing at infinity) are characterized by an internal slow oscillation ('breathing' effect), bearing a maximum amplitude ϕ_0 and a spatial extension (width) L, which are related by $L\phi_0 \approx \sqrt{|P/Q|} = \text{constant}$ [25, 41].

A dark-type solution (dark envelope soliton) is obtained for a negative value of the coefficient product, i.e. for $PQ < 0$ (or, here $Q > 0$). This solution represents a localized amplitude dip, i.e. a hole (a void) against an elsewhere constant amplitude (finite everywhere), modulating the fast carrier wave oscillation. These excitations may either present a vanishing potential at the origin, i.e. at $X = 0$ (black soliton), or a finite, i.e. non-zero one (gray soliton). In both cases the asymptotic values at infinity are constant and finite, i.e. non-zero. Similar to bright solitons, the maximum amplitude, and the spatial extension L of dark excitations satisfy the relation $L\phi_0 \approx \sqrt{|P/Q|} = \text{constant}$ [25, 41].

5. Numerical analysis and discussion

In this section we shall investigate the linear stability profile of the modulated amplitude, focusing on its parametric dependence on plasma parameters.

As we have seen, the dispersion coefficient P given by (C 1) is the same as the one given in [42] and does not depend on μ (the ratio of hot electron temperature to cold electron temperature) and ν (the ratio of warm electron density to cold electron density). Figure 1 shows the variation of P versus the normalized wave number k in the range of $0 \leqslant k \leqslant 1$ for different values of the normalized ion temperature σ. It is observed that P remains negative everywhere in this range and its absolute value at first increases and reaches maximum and then decreases as k increases for fixed σ. Also it is seen that an increase in the ion temperature leads to a decrease in the absolute value of P.

The sign of the nonlinear coefficient Q is presented for different values of μ and ν, in the range of $0 \leqslant k \leqslant 1$ and $0 \leqslant \sigma \leqslant 1$ in Figs. 2(a)–(d). The dashed lines split the $(k - \sigma)$ plane to left/right sections, where the nonlinearity coefficient Q is positive/negative, i.e. for which the wave packets are stable/unstable (recall that $P < 0$). For any given value of the normalized ion temperature σ, instability sets in above k_{cr}, where $Q(k = k_{cr}) = 0$ (see Sec. 3). Upon inspection of Figs. 2(a)–(d) we note that increasing the value of μ, for a given value of ν, leads to a decrease of the stable region in the sense that instability occurs at lower k, for higher μ. Increasing the hot component concentration, therefore, seems to destabilize a wave packet easily.

It is observed that if one keeps a fixed value of μ and increases the density ratio ν, the instability threshold (the separatrix between the two regions in the contour plots) at first decreases to a minimum value and then increases. This behavior is

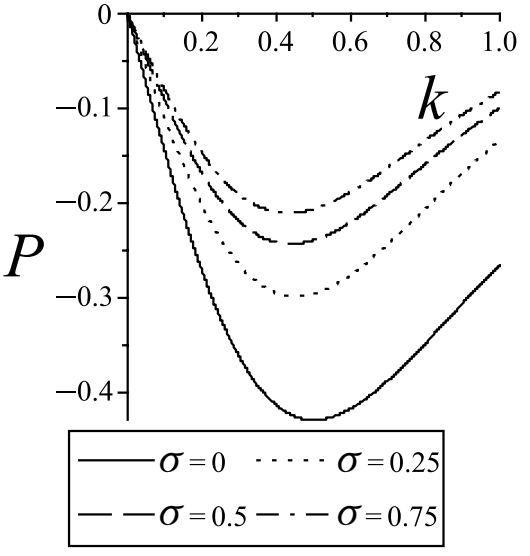

Figure 1. The dispersion coefficient P, from (C 1), is depicted against the normalized wave number k for $\sigma = 0, 0.25, 0.5$ and 0.75 (from bottom to top). The remaining plasma parameters are set to $\nu = 5$ and $\mu = 50$.

expected, since the single-electron plasma limit is realized for very high value of ν. This case falls into the same situation with $\nu = 0$ and $\mu = 1$.

For an electron-ion plasma, i.e. when $\nu = 0$ or $\nu \to \infty$ or $\mu = 1$, we obtain the same result as in [42] (cf. Figs. 2(a)–(d) here Fig. 1 in [42]). In the cold-ion limit ($\sigma = 0$), we remark that the k_{cr} first decreases and reaches a minimum value and then increases as ν increases (for fixed μ), which is in agreement with the result given in [27].

Finally, a much different behavior is witnessed for slightly larger values of μ and ν, as the instability occurs at very small wave numbers for non-zero values of σ (see Fig. 2(d)).

The nonlinear coefficient Q, given in (C 2), is depicted against the normalized wave number k for cold plasma $\sigma = 0$ in Fig. 3. The remaining plasma parameters are set to $\nu = 0, 1, 5, 10, 50$ and $\mu = 5$. Our purpose is two-fold here, namely to point out the effect of ν (disregarding thermal effects), and also to compare to earlier results [43,44] for the critical value of k, i.e. the root of Q, where the system becomes unstable. It is remarked that Q becomes zero at $k_{cr} \approx 1.47$ (for $\nu = 0$, i.e. in the *e-i* plasma limit), which is in perfect agreement with the results given in [43,44]. It may be added that such a higher wave number is admittedly invalidated by Landau damping (overseen in the fluid description), yet the analysis is being provided here for the sake of reference, thus confirming the validity of our algebraic calculation via a comparison to existing results.

Let us now consider the envelope soliton width L, which depends on the P and Q coefficients as $L^2 \approx |P/Q|$ (see the previous section). Figure 3 shows the ratio P/Q versus k for fixed values of μ and ν, and for three different values of σ. It is seen that the width of dark/bright envelopes increases/decreases as k increases. As a general conclusion, both the range of existence and the characteristics of bright/dark envelope excitations can be deduced from Figs. 1–3. The area near

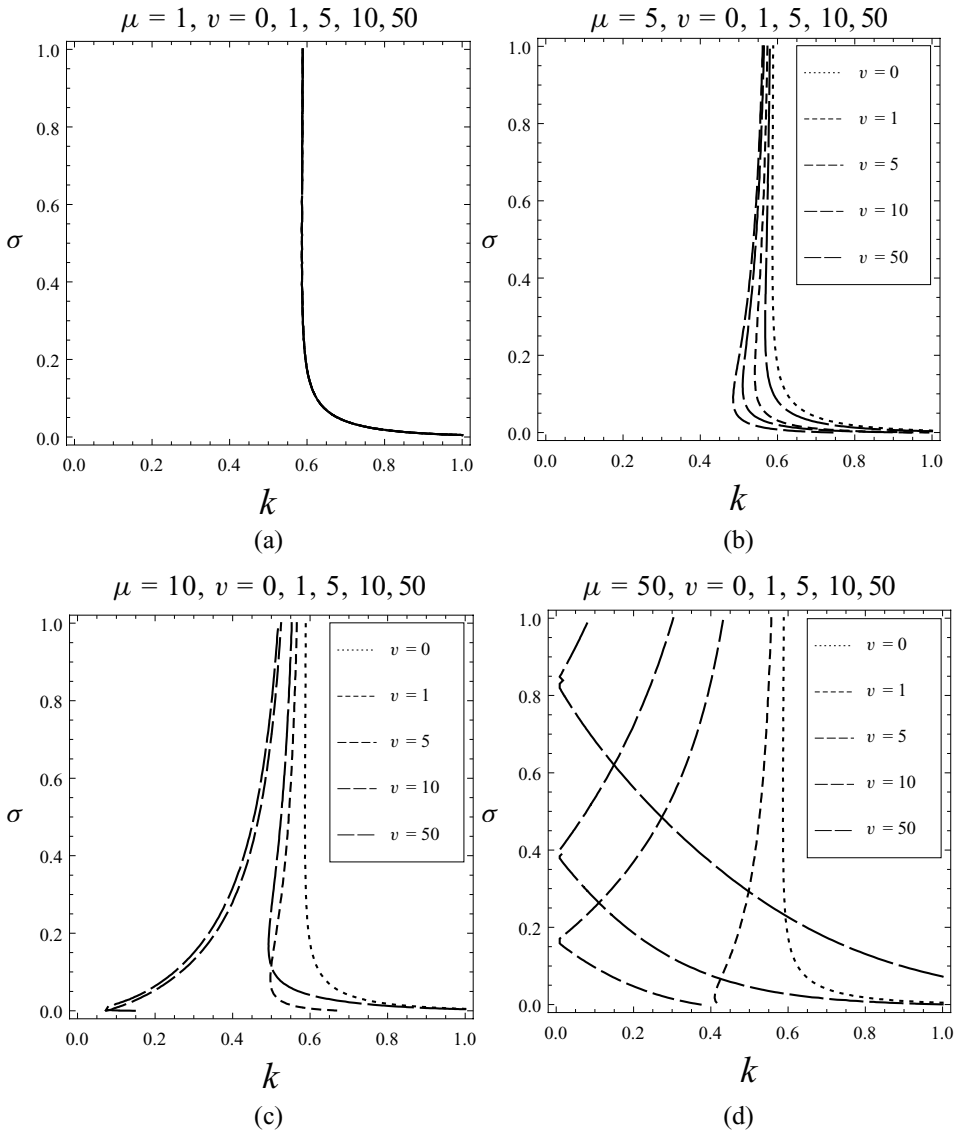

Figure 2. The $Q = 0$ contour is shown in the plane of the normalized wave number ($k = r_D/\lambda$) versus the normalized ion-temperature σ. The dashed lines in each plot (a, b, c, d) split the $\sigma - k$ plane into left/right regions, in which Q possesses positive/negative values, i.e. the region in which modulational stability/instability is predicted and, independently, wherein dark/white-type solitary excitations may exist. The hot-to-cold electron temperature ratio $\mu = T_h/T_c$ here is fixed for each plot, while different values of the hot-to-cold electron density ratios ($\nu = 0$, 1, 5, 10, 50) are considered. Top left: (single-temperature) electron-ion limit provided, for comparison; top right: $\mu = 5$; bottom left: $\mu = 10$; bottom right: $\mu = 50$.

the threshold $k = k_{cr}$ is worth a further comment: as we approach the boundary separating the left from the right region(s) in Figs. 2, the width of envelope solitons increases (see Fig. 3) as Q approaches zero near the threshold $k = k_{cr}$. The model employed here fails in that region, as higher-than-cubic nonlinearity needs to be taken into account on a different dynamics scale (not our scope here).

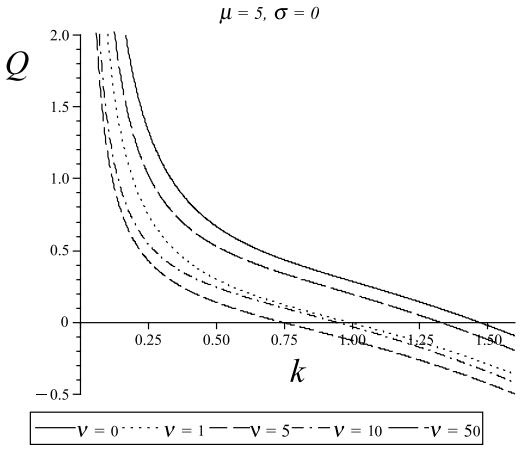

Figure 3. The nonlinear coefficient Q, from (C 2), is depicted against the normalized wave number k for $\sigma = 0$. The remaining plasma parameters are set to $\nu = 0, 1, 5, 10,$ and 50 and $\mu = 5$.

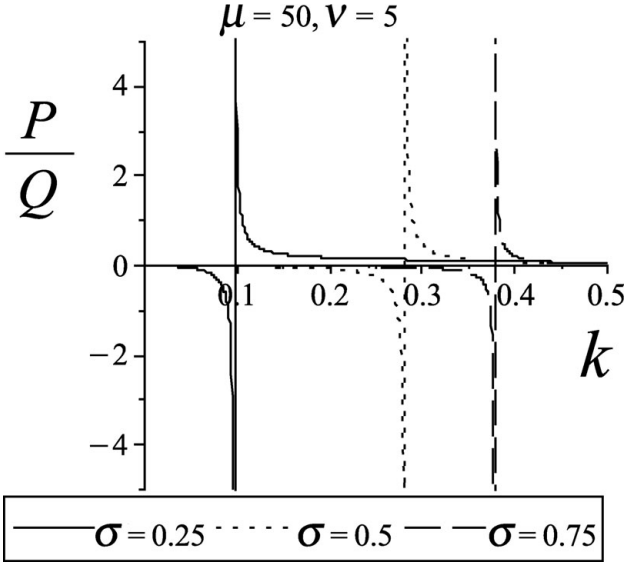

Figure 4. The coefficient ratio P/Q is shown versus the carrier wave number k, for fixed values of electron density ($\nu = 5$), electron temperature ratio ($\mu = 50$) and for different values of ion-temperatures. The different curves correspond to different values of σ ($\sigma = 0.25, 0.5$and 0.75). Recall that the sign P/Q determines the type of envelope soliton, while its absolute value determines its width for given maximum amplitude (or vice versa).

6. Conclusions

We have investigated the amplitude modulation of IAW in 2eT plasmas. The set of fluid equations was reduced to a NLSE using a multiple-scales perturbation technique. The possibility of occurrence of modulated solitary envelope structures modeled as solutions of the NLSE was studied. The linear stability analysis for

the amplitude, based on the NLS, has shown that waves will be stable/unstable for small/large wave numbers, also depending on relevant plasma parameters (ion-temperature σ, hot-to-cold electron temperature μ, and density ν).

We have pointed out the existence of a critical wave number (whose value depends on μ and ν), beyond which instability sets in. Moreover, we have shown that an increase in the value of μ, for a given value of ν, leads to the stability region being reduced (i.e. modulation instability (MI) occurring at lower k). A different behavior is met for large values of μ, ν and at certain non-zero values of σ, enabling MI to occur at very small wave numbers, i.e. enhancing instability. Wave packets are always modulationally stable in the long wavelength limit. It was shown that increasing the value of the hot-to-cold electron temperature ratio (μ) for a given value of the hot-to-cold electron density ratio (ν) favors instability. This subtle mechanism also depends on the ion temperature. The density and temperature ratio(s) of the two electron populations thus appear to control instability and tune the formation of envelope solitons.

It may be added, for rigor, that Landau damping, which is inevitably neglected when using a fluid model, should in principle impede wave propagation for large k. A kinetic description might certainly be a wiser approach in this case, for shorter wavelengths, yet lies beyond our scope in this article.

Acknowledgements

The work of IK was supported by a UK EPSRC Science and Innovation award to QUB/CPP (grant EP/ D06337X/1).

Appendix A. Second-order second harmonic amplitudes (n = 2, l = 2)

The second-order ($n = 2$) second harmonic ($l = 2$) contribution amplitudes involve a set of coefficients – see (3.8) – which are presented below.

$$\Phi_{2,2} = \frac{k^2(\omega^2 + k^2\sigma)}{2(\omega^2 - 3k^2\sigma)^3} - \frac{\alpha}{3k^2},$$

$$N_{2,2} = \frac{3k^4(\omega^2 + k^2\sigma)}{2(\omega^2 - 3k^2\sigma)^3} + \frac{k^2\Phi_{2,2}}{(\omega^2 - 3k^2\sigma)},$$

$$U_{2,2} = \frac{k^3\omega(\omega^2 + 9k^2\sigma)}{2(\omega^2 - 3k^2\sigma)^3} + \frac{k\omega\Phi_{2,2}}{(\omega^2 - 3k^2\sigma)},$$

$$P_{2,2} = \frac{k^4(15\omega^2 - 9k^2\sigma)}{2(\omega^2 - 3k^2\sigma)^3} + \frac{3k^2\Phi_{2,2}}{(\omega^2 - 3k^2\sigma)}\,.$$

Appendix B. Second-order zeroth harmonic amplitudes (n = 2, l = 0)

The second-order zeroth harmonic coefficients in (3.9) are given below:

$$\Phi_{2,0} = -\frac{\omega^2k^2 + 2\lambda k^3\omega + 3k^4\sigma + 2\alpha(\omega^2 - 3k^2\sigma)^2(3\sigma - \lambda^2)}{(3\sigma - \lambda^2 + 1)(\omega^2 - 3k^2\sigma)^2},$$

$$N_{2,0} = -\frac{k^2\omega^2 + 2k^3\omega^2\lambda + 3k^4\sigma}{(3\sigma - \lambda^2)(\omega^2 - 3k^2\sigma)^2} - \frac{\Phi_{2,0}}{(3\sigma - \lambda^2)},$$

$$U_{2,0} = -\frac{\lambda k^2\omega^2 + 6k^3\omega\sigma + 3k^4\lambda\sigma}{(3\sigma-\lambda^2)(\omega^2-3k^2\sigma)^2} - \frac{\lambda\Phi_{2,0}}{(3\sigma-\lambda^2)},$$

$$P_{2,0} = -\frac{6k^4\lambda^2 - 9k^4\sigma + 2k^3\lambda\omega + 3k^2\omega^2}{(3\sigma-\lambda^2)(\omega^2-3k^2\sigma)} - \frac{3\Phi_{2,0}}{(3\sigma-\lambda^2)}.$$

Appendix C. NLSE coefficients

The dispersion coefficient P and the nonlinear coefficient Q in the NLSE (3.10) are given as

$$P = -\frac{(\omega-k\lambda)^2(3\lambda k\omega^2 - 9\sigma\omega k^2 + 3\sigma\lambda k^3 - \omega^3)}{2k^2(\omega^2-3k^2\sigma)^3} - \frac{(\omega-k\lambda)}{2k^2}, \tag{C 1}$$

$$Q = \frac{(\omega-k\lambda)}{2k^2}(2\alpha(\Phi_{20}+\Phi_{22}) + 3\alpha') - \frac{k(\sigma kC_1 + \omega C_2)}{\omega(\omega^2-3k^2\sigma)} - \frac{C_3}{\omega}. \tag{C 2}$$

The expressions for C_1, C_2 and C_3 appearing in Q are given by

$$C_1 = k(-U_{1,1}P_{2,2} + U_{2,0}P_{1,1} + 5U_{2,2}P_{1,1} + 3U_{1,1}P_{2,0}),$$

$$C_2 = -\omega(2N_{1,1}U_{2,2} + N_{2,0}U_{1,1} - N_{2,2}U_{1,1}) + k(U_{1,1}^2N_{1,1} + U_{1,1}U_{2,2} + U_{2,0}U_{1,1} + 2N_{1,1}\Phi_{2,2} + N_{2,0} - N_{2,2}),$$

$$C_3 = k(N_{1,1}U_{2,0} + N_{2,0}U_{1,1} + N_{2,2}U_{1,1} + N_{1,1}U_{2,2}).$$

References

[1] Olsen, N. A. and Lee, Y. C. 1974 *Phys. Rev. Lett.* **33**, 1539.

[2] Jones, W. D., Lee, A., Gleman, S. M. and Doucet, H. J. 1975 *Phys. Rev. Lett.* **35**, 1349.

[3] Sudan, R. N. 1973 *Proceedings of VI European Conference on Controlled Fusion and Plasma Physics*, Vol. 2. USSR Academy of Science, Moscow.

[4] Morales, G. J. and Lee, Y. C. 1974 *Phys. Rev. Lett.* **33**, 1539.

[5] Krall, N. A. and Trivepiece, A. W. *Principles of Plasma Physics*. New York: McGraw Hill.

[6] Ergun, R. E., et al. 1998 *Geophys. Res. Lett.* **25**, 2061; Delory, G. T., Ergun, R. E., Carlson, C. W., Muschietti, L., Chaston, C. C., Peria, W., McFadden, J. P. and Strangeway, R. 1998 *Geophys. Res. Lett.* **25** 2069; Pottelette, R., Ergun, R. E., Treumann, R. A., Berthomier, M., Carlson, C. W., McFadden, J. P. and Roht, I. 1999 *Geophys. Res. Lett.* **26**, 2629.

[7] McFadden, J. P., Carlson, C. W., Ergun, R. E., Mozer, F. S., Muschietti, Roht, I. and Moebius, E. 2003 *Geophys. Res.* **108**, 8018.

[8] Temerin, M. 1982 *Phys. Rev. Lett.* **48**, 1175.

[9] Boström, R. 1988 *Phys. Rev. Lett.* **61**, 82.

[10] Berthomier, M., Pottelette, R. and Malinger, M. 1998 *J. Geophys. Res.* **103**(A3), 8261.

[11] Matsumoto, H., Kojima, H., Omura, Y., Nagano, I. and Pickett, J. S. 1998 *J. Geophys. Res.* **25**, 1277; Cattell, C. A., Dombeck, J., Wygant, J. R., Hudson, M. K., Mozer, F. S., Kletzing, M. A., Russell, C. T. and Pfaff, R. F. *J. Geophys. Res.* **26**, 425.

[12] Taniuti, T. and Yajima, N. 1969 *J. Math. Phys.* **10**, 1346; Asano, N., Taniuti, T. and Yajima, N. 1969 *J. Math. Phys.* **10**, 2020.
[13] Tagare, S. G. 1973 *Plasma Physics* **15**, 1247.
[14] Tran, M. Q. 1979 *Physica Scripta* **20**, 317.
[15] Ikezi, H. 1973 *Phys. Fluids* **16**, 1668.
[16] Lonngren, K. E. 1998 *Optical and Quantum Electronics* **30**, 615.
[17] Goswami, B. N. and Buti, B. 1976 *Phys. Lett.* **A57**, 149.
[18] Sayal, V. K., Yadav, L. L. and Shamara, S. R. 1993 *Phys. Scr.* **47**.
[19] Yadav, L. L., Tiwari, R. S. and Shamara, S. R. 1995 *Phys. Rev.* E **52**.
[20] Rao, N. N. and Shukla, P. K. 1997 *Phys. Plasmas* **4**.
[21] Chatterjee, P. and Roychoudhury, R. 1997 *Can. J. Pys.* **75**.
[22] Nishihara, K. and Tajiri, M. 1981 *J. Phys. Soc. Japan* **50**, 4047.
[23] Yadav, L. L. and Sharma, R. S. 1990 *Phys. Lett.* **150A**, 397.
[24] Mamun, A. A. and Cairns, R. A. 1996 *J. Plasma Phys.* **56**, 157.
[25] Kourakis, I. and Shukla, P. K. 2005 *Nonlin. Proc. Geophys.* **12**, 407.
[26] Sulem, P. and Sulem, C. 1999 *Nonlinear Schrödinger Equation*. Berlin, Germany: Springer-Verlag.
[27] Sharma, A. S. and Buti, B. 1978 *Pramana* **10**, 629.
[28] Kourakis, I. and Shukla, P. K. 2003 *J. Phys. A*, *Math. Gen.* **36**, 11901.
[29] Kourakis, I. and Shukla, P. K. 2004 *Phys. Plasmas* **11**, 4506.
[30] Esfandyari-Kalejahi, A. and Asgari, H. 2005 *Phys. Plasma* **12**, 102302.
[31] McKenzie, J. F., Verheest, F., Doyle, T. B. and Hellberg, M. A. 2005 *Phys. Plasmas* **12**, 102305.
[32] McKenzie, J. F., Doyle, T. B., Hellberg, M. A. and Verheest, F. 2005 *J. Plasma Phys.* **71**, 163.
[33] Cattaert, T., Verheest, F. and Hellberg, M. A. 2005 *Phys. Plasmas* **12**, 42901.
[34] Dae-Han Ki and Young-Daejung 2007 *J. Plasma Phys.* **73**, 433.
[35] Lazarus, I. J., Bharuthram, R. and Hellberg, M. A. 2008 *J. Plasma Phys.* **74**, 519.
[36] Rios, L. A., Shukla, P. K. and Serbeto, A. 2009 *J. Plasma Phys.* **75**, 3.
[37] Singh, S. V., Reddy, R. V. and Lakhina, G. S. 2001 *Adv. Space Res.* **28**, 1643.
[38] Singh. S. V. and Lakhina, G. S. 2001 *Planet. Space Res.* **49**, 107.
[39] Kourakis, I. and Shukla, P. K. 2004 *Phys. Rev.* E **69**, 036411.
[40] Shukla, P. K., Hellberg, M. A. and Stenflo, L. 2003 *J. Atmosph. Solar-Terrestrial Phys.* **65**, 355.
[41] Fedele, R., Schamel, H. and Shukla, P. K. 2002 *Phys. Scr.* T **98**, 18.
[42] Xue Ju-Kui, Duan Wan-Shan and Lang He, 2002 *Chin. Phys. Soc.* **11**, 1184.
[43] Kakutani, T. and Sugimoto, N. 1974 *Phys. Fluids* **17**, 1617.
[44] Kourakis, I. and Shukla, P. K. 2003 *Phys. Plasma* **10**, 3459.